Available online at www.sciencedirect.com
SCIENCE DIRECT®
Chemical Physics Letters 422 (2006) 256–261
CHEMICAL PHYSICS LETTERS
www.elsevier.com/locate/cplett

Furan and thiophene in liquid phase: An X-ray and molecular dynamics study

Lorenzo Gontrani [a], Fabio Ramondo [b], Ruggero Caminiti [c,*]

[a] C4T S. C. a r. L., Università di Roma, 'Tor Vergata', V. d. ricerca scientifica, I-00133 Roma, Italy
[b] Dipartimento di Chimica, Ingegneria Chimica e Materiali, Università dell'Aquila, Loc. Coppito, I-67100 L'Aquila, Italy
[c] Dipartimento di Chimica, Università di Roma, 'La Sapienza', P. le Aldo Moro 5, I-00185 Roma, Italy

Received 21 January 2006; in final form 7 February 2006
Available online 28 February 2006

Abstract

The structure of Furan and thiophene neat liquids is discussed. Energy dispersive X-ray diffraction spectra were successfully interpreted with molecular dynamics models. A detailed description of liquids at molecular level is obtainable, provided that a suitable and complete all-atom force field is employed.

1. Introduction

Furan (C_4H_4O) and thiophene (C_4H_4S) are two of the simplest etheroaromatic analogues of benzene. As in the case of pyrrole, the other member of the family of monosubstituted unsaturated five-atom ring molecules, 'aromaticity' is provided by conjugation of the unpaired p-electrons of carbon atoms and one lone pair of N, O or S atoms.

Furan can be obtained from wood oils. It is used as a solvent as well as in the synthesis of furfural and other organic compounds. It is converted to one of the most important solvents, tetrahydrofuran (THF) by hydrogenation. Furan is also used in the formation of lacquers, and in the production of agricultural chemicals (insecticides), stabilizers, and pharmaceuticals [1]. From the polymerization of furan derivatives, thermosetting resins (furan resins) are obtained. The furan ring within the resin structure provides very high resistance to chemicals. Sulfur-substituted furan derivatives are used as flavouring agents; the importance of furan fatty acids in the diet has recently been reported [2].

Thiophenes, as well, are recurring building blocks in organic chemistry [3], with applications in pharmaceuticals and electronic materials (e.g. polythiophene)[4]; their importance as biosensors has recently been reported [5].

The molecular structure of furan was investigated by gas-phase electron diffraction [6], rotational spectroscopy [7], vibrational spectroscopy in liquid and solid phase [8–10], NMR in liquid crystal [11], and inelastic neutron scattering [12]; some of these studies required theoretical calculations to interpret experimental data. A few works describe high-level ab initio calculations only [13,14]; theoretical studies of liquid furan have been reported [15].

Fewer experimental [6,7,10] or theoretical [13] studies dealt with structure determination of thiophene.

In a recent Letter [16], we demonstrated that structure function and radial distribution function of pyrrole neat liquid obtained from EDXD (energy dispersive X-ray diffraction) could be readily interpreted with molecular dynamics to derive a plausible model of the structure; the method was applied to pyrrole homologous in the present study.

2. Experimental

2.1. Sample preparation

Liquid furan (melting point: −85.6 °C, boiling point: 31.4 °C, density = 0.936 kgL^{-1}) and thiophene (melting

* Corresponding author. Fax: +39 06490631.
E-mail address: r.caminiti@caspur.it (R. Caminiti).

0009-2614/$ - see front matter © 2006 Elsevier B.V. All rights reserved.
doi:10.1016/j.cplett.2006.02.069

point: − 38 °C, boiling point: 84 °C, density = 1.051 kgL^{-1}) were purchased from Aldrich.

2.2. X-ray diffraction: data treatment

We performed our experiments using the non-commercial energy-scanning diffractometer built in the Department of Chemistry, Rome University. Detailed description of both instrument and technique can be found elsewhere [17–20]. The experimental protocol (instrument geometry and scattering angles) of the data acquisition phase is analogous to that used for pyrrole [16]. The appropriate measuring time (i.e. number of counts) was chosen so as to obtain scattering variable (q) spectra with high signal to noise ratio (500,000 counts on average). The expression for q is:

$$q = \frac{4\pi \sin\theta}{\lambda} = E \cdot 1.014 \sin\theta, \tag{1}$$

when E is expressed in keV and q in Å^{-1}. The various angular data were processed according to the procedure described in the literature [21–23] and in a few Letters from our group [17,19,20], normalized to a stoichiometric unit of volume containing one C atom and combined to yield the total '(static) structure function', $I(q)$, which is equal to:

$$I(q) = I_{\text{e.u.}} - \sum_{i=1}^{n} x_i f_i^2, \tag{2}$$

where f_i are the atomic scattering factors, x_i are the number concentrations of i-type atoms in the stoichiometric unit and $I_{\text{e.u.}}$ is the observed intensity in electron units (electrons^2). Fourier transformation of $I(q)$ led to radial distribution functions (RDF)

$$D(r) = 4\pi r^2 \rho_0 + \frac{2r}{\pi} \int_0^{q_{\max}} qI(q)M(q) \sin(rq) \mathrm{d}q \tag{3}$$

In this equation, ρ_0 (in electrons^2/Å^3) is the bulk numer density of stoichiometric units and

$$M(q) = \frac{f_C^2(0)}{f_C^2(q)} \exp(-0.01q^2) \tag{4}$$

is the sharpening factor. We used the value of 17 Å^{-1} as the upper limit of integration.

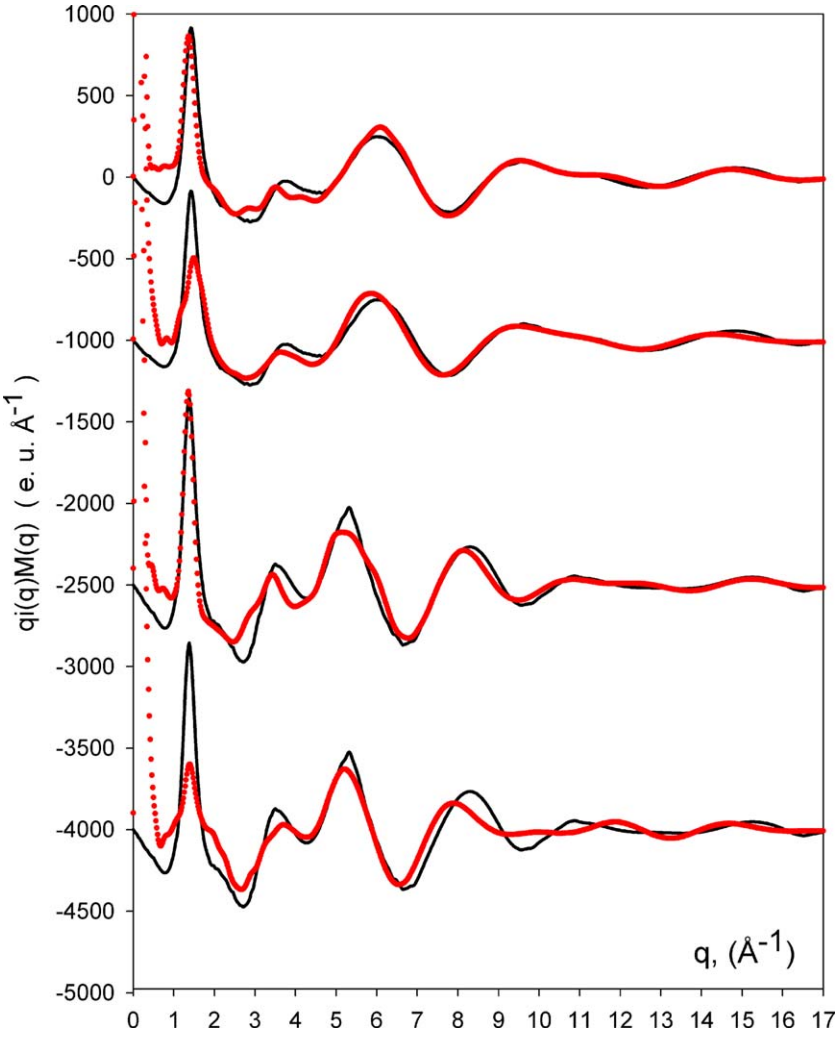

Fig. 1. Experimental structure functions – black versus theoretical functions – red. I: furan (MMFF94x); II: furan (GAFF); III: thiophene (MMFF94x); IV thiophene (GAFF). (For interpretation of the references to the color in this figure legend, the reader is referred to the web version of this article.)

3. Results and discussion

3.1. X-ray diffraction: structure functions and RDF

The measured structure functions at 25 °C (in the form $qI(q)M(q)$) for furan and thiophene are reported in Fig. 1. (Furan: I–II; thiophene: III–IV; note that the baseline is down-shifted to accommodate all the curves in a single picture and facilitate comparison); in Fig. 2 (Furan) and Fig. 3 (thiophene) radial distribution functions (in the form $\mathrm{Diff}(r) = D(r) - 4\pi r^2\rho_0$), are reported. In all the figures, experimental data are plotted in black, while model functions are in red. (Two model functions are shown: MMFF94X Fig. 1: I and III; Figs. 2 and 3: top and GAFF Fig. 1: II and IV; Fig. 2 and 3: bottom – see models). As it can be seen from the pictures, both liquids are significantly 'ordered', since they show well resolved peaks in the functions. Peak positions are reported in Table 1. In fact, in $I(q)$ function, the 'principal peak', which is attributed to long-range interactions and occurs at 1.42 Å^{-1} for furan and 1.38 Å^{-1} for thiophene, is followed by three less intense peaks. It is noteworthy that peaks are sharper, more intense and that they occur at lower q values (about 0.3–0.5 Å^{-1}) in thiophene $I(q)$. The Fourier transform of $I(q)$ (from 'reciprocal space' to 'direct space') confirms the higher stiffness of thiophene. The Diff(r) curve shows, in fact, four well-resolved peaks besides the first two ones (intramolecular interactions) for both molecules (see Fig. 1), but in the case of thiophene, a small shoulder is evident at 4.0 Å and all the peaks are shifted (0.5 Å on average) towards higher values of r. This fact can be qualitatively explained in terms of stronger dispersion interactions by sulfur atoms with respect to oxygen atoms, and accounts for higher melting and boiling points in thiophene.

3.2. Models

Model building was carried out according to the procedure described in [16], using two distinct all-atom force fields: MMFF94X Merck force field [24] and the General AMBER force field (GAFF) [25]. (see the references, MOE manual [26] or Mackerell webpage [27]) for detailed force field functional form. The protocol can be outlined as follows:

- Furan and thiophene molecules ('cleaned' by a simple builder) were first replicated in three dimensions, using the routine 'solvatebox' of leap (AMBER) [28]. Two 'pseudo-crystals' of 39 (furan) and 53 (thiophene) molecules were obtained, respectively (the different number of molecules is due to the default values of the 'bounding' box volumes for oxygen and sulfur in the program leap).
- After topology (starting structure and atom types) definition, AM1 point charges were calculated with MOPAC software [29] in the GAFF case, while no calculation was needed for MMFF94X model, since charges are automatically assigned by the software used (MOE [26]).

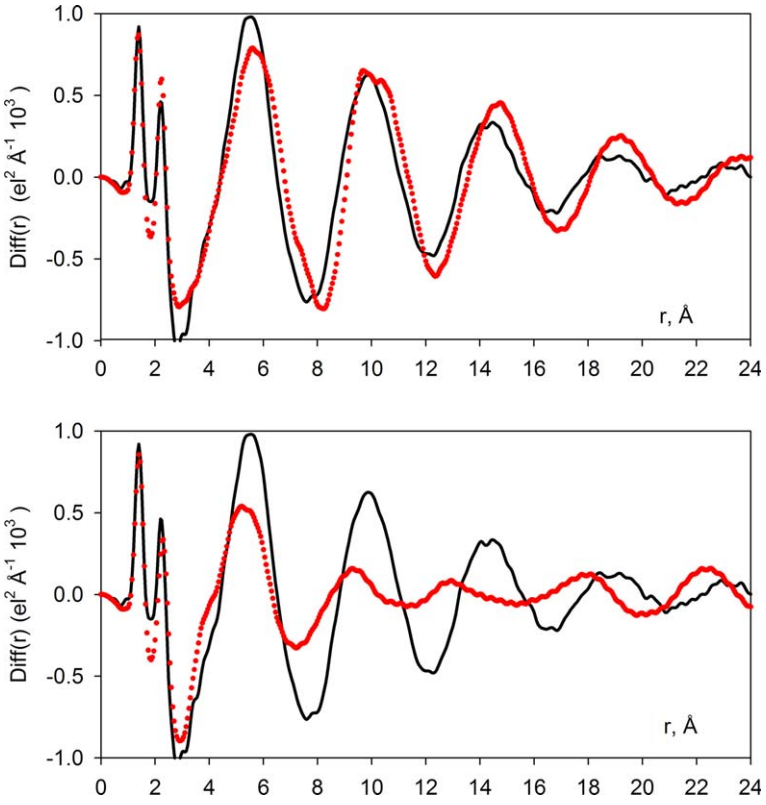

Fig. 2. Furan radial distribution functions (Diff(r)) – black versus theoretical functions – red. Top: MMFF94X; Bottom: GAFF. (For interpretation of the references to the color in this figure legend, the reader is referred to the web version of this article.)

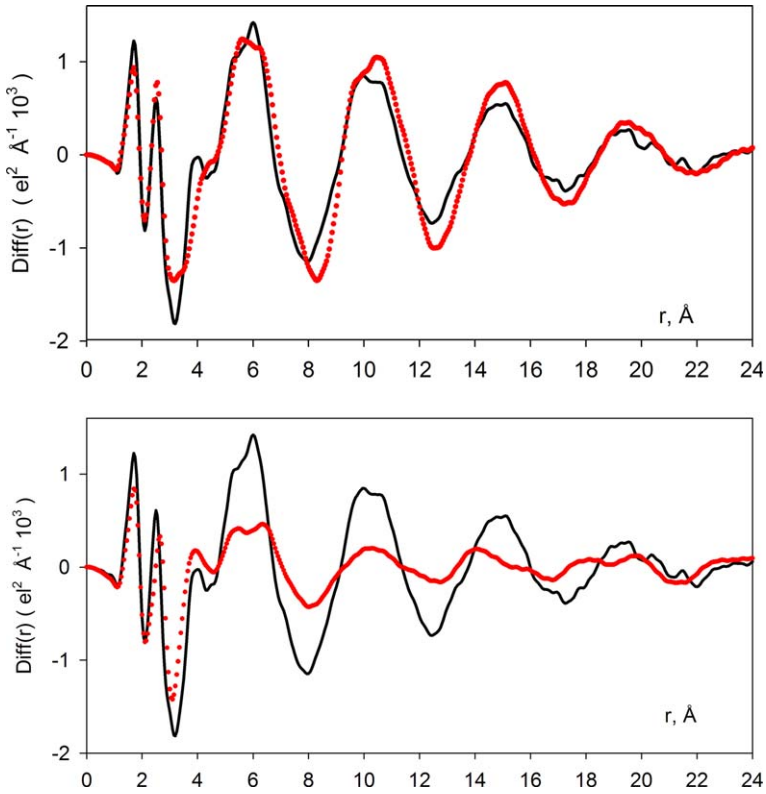

Fig. 3. Thiophene radial distribution functions (Diff(r)) – black versus theoretical functions – red. Top: MMFF94X; Bottom: GAFF. (For interpretation of the references to the color in this figure legend, the reader is referred to the web version of this article.)

Table 1
Experimental Structure function $I(q)$ (top) and radial distribution (bottom) principal peaks

Furan	Thiophene
q (Å^{-1})	
1.42	1.38
3.80	3.50
6.00	5.32
9.62	8.30
14.82	15.26
r (Å)	
4.00 (hump)	4.00
5.55	6.00
9.90	10.10
14.45	15.10
19.15	19.55

- The structure was first minimized up to a gradient of 0.05 and then simulated with molecular dynamics (MD). A trajectory of 1100 ps (100 ps heating+1000 ps production) in NVT *ensemble* was produced, with coordinates dumping every picosecond (1100 frames in total). Both values are enough to get a good agreement with experimental data. No periodic boundary conditions were applied, and SHAKE algorithm was used throughout all the simulation.
- For every dumped configuration, a model structure function was calculated, according to the Debye equation for pairs of interactions:

$$i_{mn}(q) = \sum f_m f_n \frac{\sin(r_{mn}q)}{r_{mn}q} \exp\left(-\frac{1}{2}\sigma_{mn}^2 q^2\right) \quad (5)$$

- The same sharpening factor, the same q_{max} value as for experimental data were used. σ_{mn} factors are normally added to the calculation to account for thermal fluctuations in the interatomic distance which result in peak broadening. The same σ values are generally attributed to distances falling within predefined ranges (see, for instance, [17]). Since we used molecular dynamics (which simulates the evolution of the system at a given temperature, and incorporates such effect) to build our models, all σ_{mn} values were put equal to zero. All the model functions of the configurations sampled during 'production' phase (i.e. the 1000 ps after heating) were averaged, thus obtaining a single *ensemble* structure function. The curve was extrapolated to zero below 1.1 Å^{-1} using experimental data, and then Fourier transformed into the model radial distribution function ('theoretical peaks').

Model curves are reported in Fig. 1–3. As it can be seen in Fig. 1, the structure functions $I(q)$ obtained from the molecular dynamics trajectories are both able to fit the experimental data after the principal peak, but only the MMFF94X models reproduce the 'direct space' curves (Figs. 2 and 3) after the two molecular peaks (low r values). In fact, as a general rule, it can be stated that accurate reproduction of the $I(q)$ principal peak is needed to

correctly describe long range interactions. An 'empty' peak leads to too short distance peaks in RDF (Figs. 2 and 3, bottom). MMFF94X model (top), gives an overall good reproduction of peak positions, shapes and intensities. Visual inspection of GAFF trajectory snapshots confirmed the observation that the molecules are too close to each other, while the analogous MMFF94X images show a complex aggregate of interacting molecules at great distance. This result is compliant with the existence of C—H···π, C—H···O, and H···H interactions between adjacent molecules, already described in a recent inelastic scattering experiment in solid furan [12].

In Fig. 4, two pictures of the 'transient' configuration generated during MD run are shown. The snapshots shown correspond to step #500 (half trajectory). As it can be seen, the furan aggregate (top) is more 'compact' than thiophene one. The molecules can roughly be inscribed into a cell (centered in the center of mass of the system) of dimension $20 \times 20 \times 20$ (cubic angstroms) while the dimension is $30 \times 30 \times 30$ for thiophene.

4. Conclusion

In this work, we report the application of the previously described EDXD/MD method [16] to two aromatic molecular liquids, furan and thiophene. Both liquids show a fair complexity in their long-range structure; the measured structure functions and distribution functions are well reproduced by molecular dynamics simulations with MMFF94X, a complete and widely tested force field.

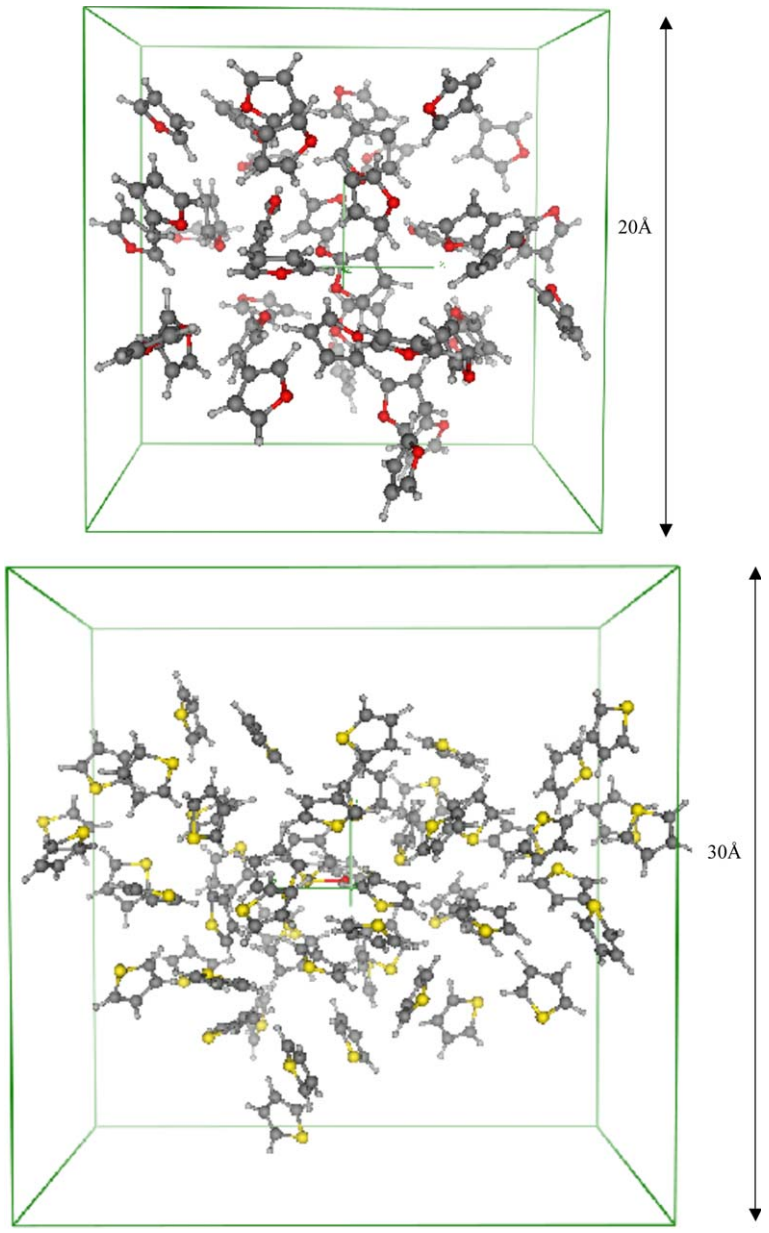

Fig. 4. Comparison between the two molecules configurations at half trajectory: furan (top), thiophene (bottom).

Poorer agreement was found using another force field, GAFF. The superior behavior of MMFF94X was noticed in the pyrrole models [16], too, and can likely be ascribed to the presence of explicit atom types for pyrrole nitrogen, furan oxygen and thiophene sulfur, and to well parametrized (through high level ab initio models [27]) non-bonding terms in the force field, while GAFF lacks completely the corresponding atom types. Comparing the three etherocycles studied so far, we can state that the agreement between theory and experiment is satisfactory in all cases, in the order pyrrole $\simeq$ furan $>$ thiophene, approximately.

Anyway, the use of a complete and all-purpose force field can be regarded as mandatory for this kind of studies.

The EDXD/MD method described in this report could as well conveniently help in the parametrization process of a force field, given its high-level structural insight. Future measurements on non-aromatic molecular liquids and molten solids are planned in our lab, to further confirm the method validity, as well as to consider different theoretical techniques and force fields.

Acknowledgements

We thank CASPUR (Centro di Applicazioni di Supercalcolo per Università e Ricerca) for technical support.

References

[1] D.M. Himmel, K. Das, A.D. Clark Jr., S.H. Hughes, A. Benjahad, S. Oumouch, J. Guillemont, S. Coupa, A. Poncelet, I. Csoka, C. Meyer, K. Andries, C.H. Nguyen, D.S. Grierson, E. Arnold, J. Med. Chem. 48 (24) (2005) 7582.
[2] G. Spiteller, Lipids 40 (8) (2005) 755.
[3] W. Steinkopf Die Chemie des Tiophens. 1941, p. 61 (CA 39, 16–482).
[4] J.L. Reddinger, J.R. Reynolds, Adv. Polym. Sci. 145 (1999) 57122.
[5] D.T. McQuade, A.E. Pullen, T.M. Swager, Chem. Rev. 100 (2000) 2537.
[6] V Schomaker, L. Pauling, J. Am. Chem. Soc. 61 (1939) 1769.
[7] C.W.N. Cumper, Trans. Faraday Soc. 54 (1958) 1266.
[8] F. Billes, H. Bohlig, M. Ackermann, M. Kudra, Theochem. 672 (1-3) (2004) 1.
[9] R. Guerin, C.R. Acad. Sci 267B (3) (1968) 199.
[10] L. Jacqueline, Compt. Rend., Ser. A 262B (1) (1966) 31.
[11] Phillip B. Liescheski, David W.H. Rankin, J. Mol. Struct. 196 (1989) 1.
[12] M. Montejo, A. Navarro, J.G. Kearley, J. Vazquez, J.J. Lopez-Gonzalez, J. Am. Chem. Soc. 126 (46) (2004) 15087.
[13] A. Balbas, M.J. Gonzalez Tejera, J. Tortajada, Theochem. 572 (2001) 141.
[14] J.S. Kwiatkowski, J. Leszczynski, I. Teca, J. Mol. Struct. 426–437 (1997) 451.
[15] N.A. Macdonald, W.L. Jorgensen, J. Phys. Chem. B 102 (41) (1998) 8049.
[16] L. Gontrani, F. Ramondo, R. Caminiti, Chem. Phys. Lett. 417 (1–3) (2006) 200.
[17] L. Gontrani, R. Caminiti, L. Bencivenni, C. Sadun, Chem. Phys. Lett. 301 (1–2) (1999) 131.
[18] R. Caminiti, V. Rossi Albertini, Int. Rev. Phys. Chem. 18 (2) (1999) 263.
[19] R. Caminiti, M. Carbone, S. Panero, C. Sadun, J. Phys. Chem. 103 (47) (1999) 10348.
[20] D. Atzei, T. Ferri, C. Sadun, P. Sangiorgio, R. Caminiti, J. Am. Chem. Soc. 123 (11) (2001) 2552.
[21] Y. Murata, K. Nishikawa, Bull. Chem. Soc. Jpn. 51 (2) (1978) 411.
[22] K. Nishikawa, T. Iijima, Bull. Chem. Soc. Jpn. 57 (1984) 1750.
[23] G. Fritsch, C.N.J. Wagner, Z. Phys. B 62 (1986) 189.
[24] T.A. Halgren, J. Comput. Chem. 17 (1996) 587.
[25] J. Wang, R.M. Wolf, J.W. Caldwell, P.A. Kollamn, D.A. Case, J. Comput. Chem. 25 (2004) 1157.
[26] © 1997–2005 Chemical Computing Group Inc. All rights reserved.
[27] Available from: <http://www.psc.edu/general/software/packages/charmm/tutorial/mackerell/MMFF_00.pdf>.
[28] D.A. Case et al., AMBER 7, University of California, San Francisco, 2002.
[29] J.J.P. Stewart, MOPAC: A General Molecular Orbital Package. Quant. Chem. Prog. Exch. 10:86 (1990).